GLIA 27:101–109 (1999)

Non-Myelin-Forming Perisynaptic Schwann Cells Express Protein Zero and Myelin-Associated Glycoprotein

JOHN GEORGIOU AND MILTON P. CHARLTON*
Department of Physiology, MRC Group in Nerve Cells and Synapses and Neuroscience Network, University of Toronto, Toronto, Ontario, Canada

KEY WORDS myelin; glycoprotein; neuromuscular junction; Schwann cell; glia; nerve terminal; synapse

ABSTRACT Perisynaptic Schwann cells (PSCs) envelop axonal terminals and are physiologically distinct from the nearby myelinating Schwann cells (MSCs), which surround the same innervating motor axons. PSCs have special functions at the neuromuscular synapse, where they detect and can modulate neurotransmitter release. Although PSCs are similar to non-myelinating Schwann cells in that they do not form multiple myelin wrappings around nerve terminals, they do wrap around single nerve terminals. These differences, as well as others, lead us to question whether PSCs are truly of Schwann cell origin. We thus characterized the expression of molecules, classically associated with myelin and Schwann cells, in PSCs at the frog neuromuscular junction. We wondered whether PSCs express the Schwann cell marker protein zero (P_0) and whether their lack of myelination was related to an absence of myelin-associated glycoprotein (MAG), a protein found in myelinating cells that is considered important in myelination. Instead, we found that PSCs express both P_0 and MAG, and other myelinating glial markers such as galactocerebroside and 2′,3′-cyclic nucleotide 3′-phosphodiesterase. In denervated preparations, P_0 and MAG expression persisted, including at newly formed PSC extensions. Because PSCs do not myelinate, it is clear that expression of these proteins alone is not sufficient for myelin formation. It is possible that factors present at synapses may prevent myelination, while P_0 and MAG may mediate adhesion between nerve terminals and the surrounding PSCs. The results indicate that PSCs are of Schwann cell origin. *GLIA 27:101–109, 1999.*

INTRODUCTION

Schwann cell precursors are derived from the neural crest, and they subsequently give rise to two mature Schwann cell forms, the myelin- and non-myelin-forming Schwann cells (for review see Le Douarin et al., 1991; Jessen and Mirsky, 1991, 1998). In the adult, each myelinating Schwann cell (MSC) surrounds a single axon where it forms layers of myelin sheath. In contrast, each non-myelin-forming Schwann cell can accommodate many axons in troughs along its surface. Another type of non-myelin-forming cell can be found at the neuromuscular junction (nmj), and this cell is known as a terminal or perisynaptic Schwann cell (PSC). Each PSC wraps around portions of a single nerve terminal, and these cells have specialized functions at the nmj, where they detect synaptic activity (Jahromi et al., 1992; Reist and Smith, 1992) via activation of their neurotransmitter receptors (Robitaille, 1995; Robitaille et al., 1996, 1997; Bourque and Robitaille, 1998). The PSCs react to cessation of nerve activity (Georgiou et al., 1994, 1999) and can be activated to modulate transmitter release (Robitaille, 1998). Furthermore, PSCs also have roles in synaptic mainte-

Grant sponsor: Medical Research Council of Canada; Grant sponsor: Neuroscience Network.

*Correspondence to: Milton P. Charlton, Department of Physiology, MSB 3232, University of Toronto, 1 King's College Circle, Toronto, Ontario, Canada, M5S 1A8. E-mail: milton@spine.med.utoronto.ca

Received 10 February 1999; Accepted 17 February 1999

nance, growth, and repair (for review see Balice-Gordon, 1995; Son et al., 1996). Thus, PSCs are morphologically and functionally quite distinct from both MSCs and non-myelin-forming Schwann cells in unmyelinated nerve. Indeed, PSCs have many functions that are more similar to astrocytes than myelin- or non-myelin-forming Schwann cells (Georgiou et al., 1994).

During development of the nmj, a neuronal growth cone contacts a muscle fiber and differentiates into a specialized presynaptic nerve terminal, which becomes wrapped by Schwann cell processes (for reviews see Hall and Sanes, 1993; Burden, 1998). However, the origin of PSCs is unknown. Immunological approaches have been used to identify Schwann cells during development and also to distinguish between the adult myelin- and non-myelin-forming types of these glia (for reviews see Jessen and Mirsky, 1991, 1998; Scherer, 1997). Although the molecular profile of Schwann cells is distinct from other cell types, it is still unknown whether PSCs express any proteins that are specially associated with Schwann cells. For instance, protein zero (P_0) is a Schwann cell glycoprotein constituent, which is expressed in precursor cells and becomes up-regulated in MSCs upon myelin formation (Bhattacharyya et al., 1991; Zhang et al., 1995; for reviews see Martini and Schachner, 1997; Scherer, 1997). We wondered whether PSCs express Schwann cell markers such as P_0 and whether the absence of myelination in PSCs is due to the absence of myelin-related proteins such as myelin-associated glycoprotein (MAG).

We have determined that PSCs express proteins associated with mature Schwann cells, including P_0. Surprisingly, PSCs also expressed the myelinating cell markers MAG and 2′,3′- cyclic nucleotide 3′-phosphodiesterase (CNPase). PSCs also expressed the major myelin galactolipid and general Schwann cell marker galactocerebroside (GalC). After denervation, PSCs and their newly formed processes still contained P_0 and MAG. Our results indicate that PSCs are of Schwann cell origin and that expression of these proteins alone is insufficient for development of a myelin sheath. We postulate that neurotransmitters and other molecules found at synapses prevent myelination and lead to specialization of perisynaptic glial cells. Alternatively, P_0 and MAG may play other roles, such as neuron–glia adhesion and signaling.

MATERIALS AND METHODS

Animals and Experimental Treatment

Rana pipiens frogs (4–6 cm body length; Ward's Scientific, St. Catherines, ON, Canada or Connecticut Valley Biological Supply, Southampton, MA) were housed at 15°C in running water. Frogs were double-pithed and cutaneous pectoris muscles (Dreyer and Peper, 1974) were excised and pinned down on petri dishes coated with Sylgard (Dow Corning, Midland, MI). Preparations were maintained in normal frog Ringer's solution (FRS) containing 120 mM NaCl, 2 mM KCl, 1 mM $NaHCO_3$, 1.8 mM $CaCl_2$, 5 mM HEPES (pH adjusted to 7.2 using NaOH).

Denervation of muscles was performed in a manner similar to the method of Robitaille et al. (1996, 1997). We injected 0.3 mg/g frog body weight of MS-222 (3-aminobenzoic acid ethyl ester, methane sulfonate salt; Sigma Chemical, St. Louis, MO) dissolved in FRS into a dorsal lymphatic sac to anaesthetize frogs. Two 1 cm skin incisions were made over the cutaneous pectoris muscle. A 0.5 cm portion of the motor nerve was removed at one muscle, without damaging the vasculature. The skin was sutured using silk thread and sealed with Histoacryl blue (B. Braun Melsungen AG, Melsungen, Germany, D-3508). Frogs were maintained in individual cages for 14 days. Contralateral muscles served as controls. In this preparation, nerve terminals degenerate within several days and are phagocytosed by the PSCs (Birks et al., 1960b; Ko, 1981).

Staining and Immunohistochemistry

To identify endplates, muscles were stained with peanut agglutinin (PNA) lectin conjugated to tetramethylrhodamine isothiocyanate (PNA-TRITC; Sigma; 10 mg/ml in FRS), applied for 10 min. Protein zero (P_0) was detected with 1E8 monoclonal antibody (courtesy of Dr. Robert Brackenbury and Dr. Nancy Ratner, University of Cincinnati). This antibody is specific for myelin-and non-myelin-forming Schwann cells in mature chickens (Bhattacharyya et al., 1991) and reacts with the polypeptide portion of chicken P_0 (Zhang et al., 1995). Preparations were incubated in FRS containing 20 μg/ml 1E8 for 12–16 h (this step at 15°C), washed for 1 h in FRS, then incubated in FRS containing 10 μg/ml goat anti-mouse IgG secondary antibody conjugated to fluorescein isothiocyanate (FITC, Sigma) for 2 h, and finally rinsed for 1 h in FRS. Muscles were imaged live. No fluorescence signal was observed when the primary antibody was omitted.

Preparations processed for either MAG or GalC expression were fixed in FRS containing 3% paraformaldehyde (5°C) for 10 min and rinsed in FRS for 60 min. Monoclonal antibody (mAb) 513, originally raised against chicken brain glycoproteins (Poltorak et al., 1987) was provided by Dr. John Roder (Samuel Lunenfeld Research Institute, Mt. Sinai Hospital, Toronto, Canada). Anti-MAG (clone 3E4, ascites) was provided by Dr. Samuel David (Centre for Research in Neuroscience, Montréal General Hospital Research Institute, Montréal, Canada). GalC was detected using polyclonal antiserum from Sigma (#G-9152), or Ranscht mAb (R-mAb; Ranscht et al., 1982) from Dr. Barbara Ranscht (The Burnham Institute, La Jolla Cancer Research Center, La Jolla, CA), or mAb O1 (Sommer and Schachner, 1981) courtesy of Dr. Roder. CNPase was detected using clone 11–5B mAb (Boehringer Mannheim Canada, Laval, Québec, Canada). During the staining procedure, muscles were incubated in pairs and moved between five well plates, each containing a

solution of 10% bovine serum albumin (BSA; Sigma) and 0.3% Triton X-100 (Boehringer Mannheim) in FRS. The procedure followed these steps: (1) Preparations were "blocked" in this solution for 30 min, (2) followed by 60 min incubation with either antibody 513 (1:50) or 3E4 (1:50) or G-9152 (1:50) or O1 (1:50) or R-mAb (1:20) or 11–5B (20 μg/ml) and (3) rinsed twice for 60 min. Tissue was next (4) incubated in 10 μg/ml goat anti-mouse IgG secondary antibody conjugated to FITC, or IgM secondary (Sigma) for O-1 detection, and (5) rinsed twice for 30 min. Preparations were mounted onto glass slides in a drop of Slowfade antifade reagent (Molecular Probes, Eugene, OR) to reduce photo-bleaching. Fluorescence signal was not observed when the primary antibodies were omitted.

Muscles were imaged using a Bio-Rad 600 confocal laser scanning microscope attenuated to 1% of the full laser power. For live preparations, images were collected using a 40× water immersion lens (Nikon 0.55 NA). Fixed muscles were imaged with a 40× oil immersion lens (Nikon 1.30 NA). The dual wavelength mode of the confocal microscope allowed acquisition of green and red fluorescence simultaneously. This provided co-localization of each protein probed in double-labeled samples; in this configuration, the excitation wavelength is 514 nm and one photomultiplier tube detects green emitted light (selected using 514–550 nm band pass filter) while the other detects red light (low pass filter with 590 nm cutoff).

Immunoblots

Rat brain, frog brain, and frog peripheral nerve tissue were dissected and suspended in ice cold phosphate buffered saline containing 1% (v/v) Triton X-100 and protease inhibitors (cocktail kit from ICN Pharmaceuticals Canada Ltd, Montréal, QC, H4M 1V1) AEBSF (200 μg/ml), EDTA-Na_2 (2.5 mg/ml), leupeptin (1 μg/ml), and pepstatin A (1 μg/ml). Tissue was homogenized (Polytron) and frozen in aliquots. Protein concentrations were determined by dotMETRIC 1μl Protein Assay (Geno Technology Inc., St. Louis, MO, 63108).

Proteins were fractionated in polyacrylamide gels (bis:acrylamide of 1:37.5), which were cast and run using the Mini-PROTEAN II electrophoresis cell system (Bio-Rad Laboratories, Hercules, CA). Tissue samples were diluted with stock buffer to contain 31.25 mM Tris-HCl (pH 6.8), 1% sodium dodecyl sulfate (SDS), 5% glycerol, and 0.05% bromophenol blue. In some experiments, samples were reduced with 50 mM DTT and boiled for 10 min. Pre-stained molecular weight standards (Low Range and/or Kaleidoscope Markers; Bio-Rad) were fractionated simultaneously. Proteins were transferred onto immuno-blot polyvinylidene difluoride (PDVF) membrane (Bio-Rad) using the Bio-Rad Trans-Blot semi-dry transfer cell apparatus.

Membranes were blocked for 2 h in Tris-buffered saline/Tween-20 (TBS/T: 50 mM Tris-HCl, 150 mM NaCl, 0.1% Tween-20, pH 7.4) containing 5% (w/v) nonfat dry milk (Bio-Rad). Membranes were washed in TBS/T and then incubated with primary antibody overnight (this step at 5°C) in TBS/T solution containing 5% (w/v) BSA. Antibody solution volume was 20 ml and contained either 1E8 (6 μl), 513 (10 μl), or 3E4 (10 μl). After washing in TBS/T, PVDF membranes were incubated for 2 h in 20 ml of TBS/T milk blocking buffer containing 4 μl of horseradish peroxidase-conjugated rabbit anti-mouse IgG secondary antibodies (Sigma). Membranes were subsequently washed in TBS/T and immunoreactive bands were detected by chemiluminescence (SuperSignal chemiluminescent substrate; Pierce, Rockford, IL) and exposed to Biomax ML light film (Eastman Kodak, Rochester, NY).

RESULTS

Protein Zero Expression

The major protein in PNS myelin is P_0, a glycoprotein believed to be essential in compaction of myelin (Doyle and Colman, 1993; Quarles, 1997; Sommer and Suter, 1998). To evaluate whether P_0 is expressed in PSCs, we immunostained live, excised neuromuscular preparations using monoclonal antibody 1E8 (Bhattacharyya et al., 1991; Zhang et al., 1995).

We detected P_0 immunoreactivity on the MSCs surrounding the motor axons and also on PSCs. Staining on the MSCs located at the last myelinated segments was typically brighter than staining on PSCs (not shown). However, the larger surface area of MSCs may account for this difference in immunoreactivity, and we thus did not attempt to quantitate P_0 expression. However, the expression of P_0 by both MSCs and PSCs suggests some common role for this molecule, but one which may not necessarily relate to myelination.

The pattern of P_0 expression on PSCs predominantly formed an outline similar to that seen with fluorescent peanut agglutinin (PNA), a lectin which binds to extracellular glycosylated residues at neuromuscular synapses (Ko, 1987) and forms an outline around PSC nuclei (Georgiou et al., 1994). We examined 62 sites from 5 muscles labeled with PNA and observed a uniform, a dotted, and also a "banded" pattern of P_0 expression. Bands of P_0 staining, oriented perpendicularly to the long axis of the PSC processes, were spaced 1–2 μm apart. The PSC imaged in Figure 1A was double-labeled for P_0 and PNA, and it reveals some of these varied patterns of P_0 expression. For instance, the left portion is uniform, the portion on the right forms an outline, and the central portion of the PSC displays a banded staining pattern, which appeared brightest when focussing down towards the synaptic cleft. When the two signals were superimposed, the P_0 staining paralleled and also overlapped to a considerable extent with that of the PNA staining (overlap appears in yellow). However, the P_0 bands did not co-localize with PNA staining, as illustrated in the merged image of Figure 1A, where P_0 bands still appear green.

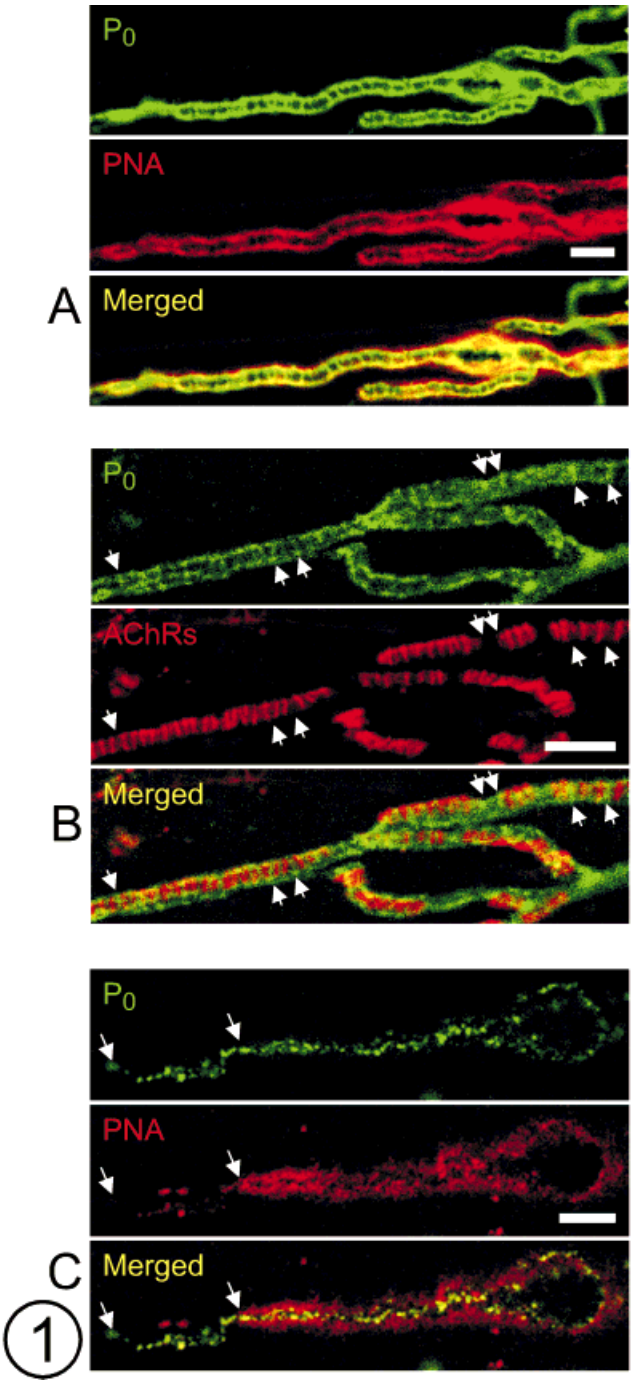

Fig. 1. PSCs express P_0. Simultaneously acquired confocal images from muscles double-labeled using anti-P_0 (1E8) revealed with goat anti-mouse FITC (**top panel**) and with either PNA-TRITC to outline synapses (**A,C**) or α-bungarotoxin-Texas Red (**B**) to reveal postsynaptic nicotinic acetylcholine receptors, AChRs (**center panel**). Green and red images are merged in the bottom panels to show any spatial overlap, which appears yellow. Scale bars = 10 μm. A: Note that the outline formed by PNA overlaps with the P_0 staining, but the P_0 bands and the fine tip (left end) of the PSC do not. B: P_0 bands are located between active zones, that is, P_0 bands (arrows) reveal little or no overlap with that of AChRs. **C:** Two weeks after denervation, PSCs still contain P_0. Note the newly formed P_0-containing extension to the left of the PNA outline (between arrows).

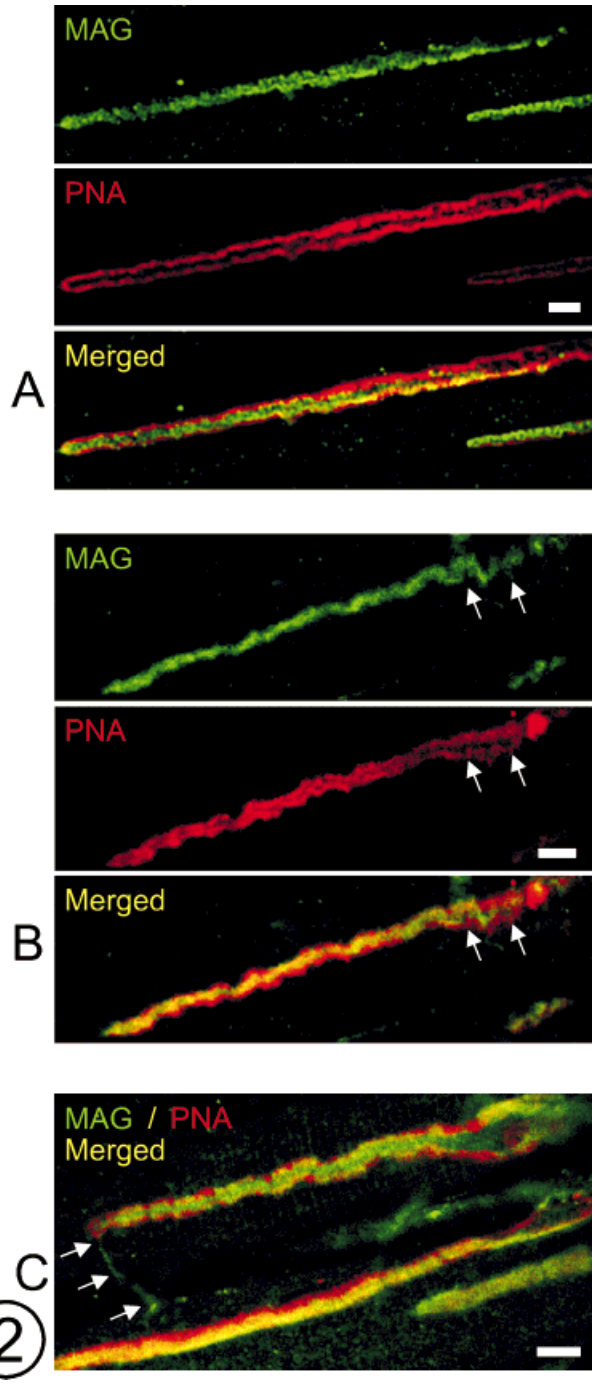

Fig. 2. MAG expression at PSCs. Simultaneously acquired confocal images of MAG (513) staining revealed with goat anti-mouse FITC and PNA-TRITC to outline synapses. Scale bars = 10 μm. **A:** PSCs covering two nerve terminals expressing MAG. **B:** Another synapse in which MAG staining meanders through but does not completely fill or outline the PSC soma region defined by PNA. **C:** Merged image showing localization of MAG (green) and PNA (red) in a PSC denervated two weeks previous to staining (overlap appears yellow). Note the PSC extension growing away from the PNA-delimited former boundary of the synapse (arrows).

Localization of P_0 Bands on PSCs

PSCs extend fine processes that wrap around the nerve terminal and are situated between some of the active zones, sites of neurotransmitter release, which occur at regularly spaced 1 μm intervals in frogs (Birks et al., 1960a; McMahan et al., 1972; Dreyer et al., 1973; Heuser and Reese, 1977). To determine whether spots and bands of P_0 correspond to PSC processes, we double-labeled synapses with fluorescent α-bungarotoxin, which binds to postsynaptic nicotinic acetylcholine receptors (AChRs) located opposite active zones (Anderson and Cohen, 1974; Robitaille et al., 1990). We hypothesized that if P_0 staining is on PSC processes, then the bands of P_0 staining should not overlap with those of AChRs.

We found that P_0 bands did not overlap with those of AChRs. An example of a synapse double-labeled for P_0 and AChRs appears in Figure 1B. Arrows point to selected regions of P_0 immunoreactivity, with the corresponding locations also shown in the image of AChR staining, as well as in the merged image. Note the lack of overlap (which would appear yellow) between the two signals, particularly for the P_0 bands, some of which are indicated by arrows. Similar staining results were seen at 50 sites from 3 muscles. The results indicate that bands of P_0 staining are between the active zones and likely represent staining at the level of PSC processes.

PSC Extensions Contain P_0

Sprouting of PSCs has been observed previously in denervated muscles of rats using antibodies against various proteins and receptors (Reynolds and Woolf, 1992; also see Discussion). To determine whether PSC extensions contain P_0, we denervated frog muscles and immunostained for P_0 two weeks later.

In denervated preparations, we observed P_0 staining in PSC processes that extended beyond the former boundaries of synapses, as delimited by PNA. These frequently appeared as either a fine (< 1 μm width), uniformly stained extension leading away and often parallel to the synapse, or also in the form of regularly spaced P_0 spots, as in Figure 1C. The distance between spots varied from about 0.7 to 2.0 μm. Similar results were seen at 41 sites from 3 muscles. Although the distribution of P_0 changed after nerve degeneration, its persistence indicates that the protein is expressed on PSCs and that not all of the immunostaining at intact synapses is located on nerve terminals. The results show that denervated PSCs contain P_0, as do their newly formed processes.

Expression of Myelin-Associated Glycoprotein

The transmembrane glycoprotein MAG is a cell adhesion molecule belonging to the immunoglobulin gene superfamily and is expressed in the periaxonal membranes of myelin-forming cells (for review see Quarles, 1997). MAG is important in modulating the structure of myelinated axons (Yin et al., 1998). Since MAG has been shown to be an important marker of MSCs, we investigated whether PSCs lack this myelin-related molecule.

Immunostaining with anti-MAG (clone 513) antibody detected MAG on both MSCs and PSCs. The images in Figure 2A are from a neuromuscular synapse double-labeled for MAG (top) and PNA (center). The MAG staining was nearly continuous and restricted primarily to within the outline formed by PNA. We found similar results in the 25 sites (4 muscles) examined. Similar staining was also observed using a different mAb against MAG (3E4; 33 sites from 3 muscles; images not shown).

The MAG immunostaining pattern probably reflects an adaxonal distribution. Besides the narrow staining pattern observed (in relation to the PNA outline), MAG staining did not widen to fill the cell body of the PSC. Instead, MAG labeling followed through the middle or along one edge of the PSC soma region. The images in Figure 2B are from a clone 513-labeled synapse in which a soma was well defined by PNA. However, the MAG antibody revealed a winding pattern of staining through the center of the soma region, which was not any wider than MAG staining at the level of the PSC processes. In 15 of 20 PSCs (from the 3 muscles) there were distinct somata outlined by PNA, and in these, MAG staining filled less than half of the soma area. While it cannot be excluded that MAG is distributed on the outer PSC membrane, the data suggest that most of the MAG is confined to the inner membrane surface which apposes the nerve terminal.

MAG Remains After Denervation

To determine whether MAG expression persists after denervation, we transected the motor nerve leading to muscles and evaluated MAG staining two weeks later. We examined 24 sites from 3 denervated muscles and found MAG at PSCs and their newly formed extensions. The merged (MAG and PNA) image in Figure 2C is from a denervated muscle and shows two PSCs containing MAG. Note that the upper PSC contains a MAG-labeled extension that leads away from the edge of a PNA-delimited former synaptic boundary (arrows). In summary, denervated PSCs and their newly formed processes express MAG. Furthermore, the data suggest that the MAG staining observed in the normal innervated preparations (Fig. 2A,B) reflects staining on PSCs, not nerve terminals.

Immunoblot Characterization of 1E8, 513, and 3E4 Antibody Reactivities

We next determined the specificity and characteristics of the proteins identified by the mAbs against P_0

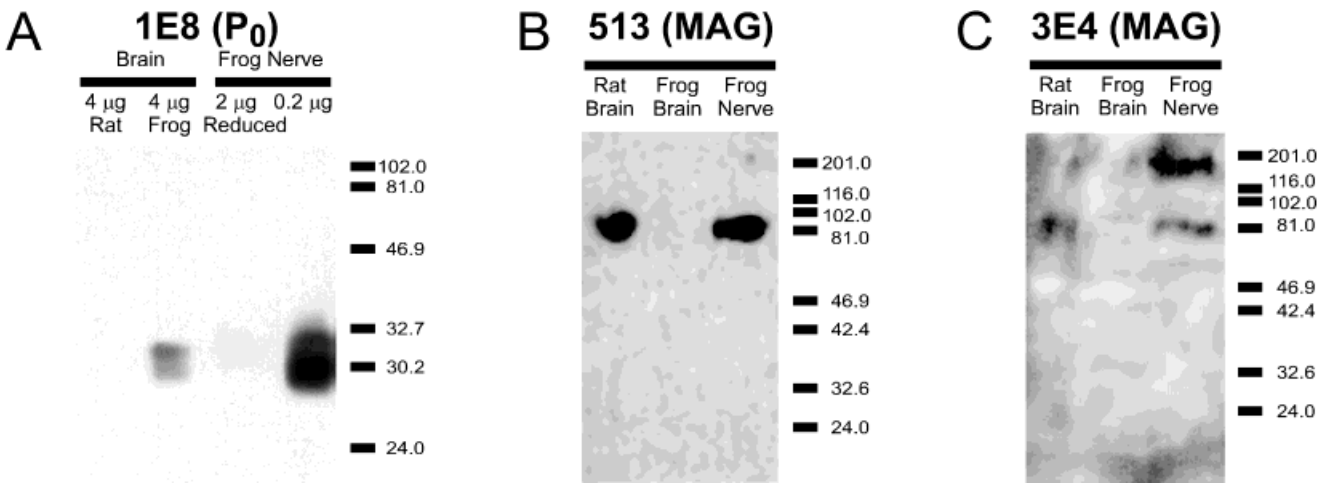

Fig. 3. Western blot analyses of antibody reactivities. Prestained molecular weight standards (migration appears in kDa) were fractionated simultaneously. **A:** Immunoblot of anti-P_0 (1E8) reactivity. Indicated amounts of homogenized rat brain, *Rana pipiens* frog brain, and frog nerve were electrophoresed on 12% SDS polyacrylamide gels. Only the sample labeled "reduced" was treated with DTT, and this eliminated most of the 1E8 binding. **B:** Immunoblot of anti-MAG (513) reactivity. Homogenized rat brain (2 µg), frog brain (80 µg) and frog nerve (80 µg) were electrophoresed on 10% SDS gels. **C:** Analysis of anti-MAG (3E4) binding. Conditions and proteins were identical to that in B.

(1E8) and MAG (513 and 3E4) in *Rana pipiens* frog brain and peripheral nerve. The 1E8 mAb, which is known to bind to native chick but not rat P_0 (Bhattacharyya et al., 1991), reacted only with non-reduced frog nerve tissue, revealing a doublet of about 30 kDa apparent mobility (Fig. 3A). There was weak staining in extract of frog brain, but none in a corresponding amount of rat brain. The results suggest that in *Rana* frogs, 1E8 binds to a protein abundant in peripheral nerve with a mobility consistent with that of P_0 (see Discussion).

The 513 mAb, which recognizes native MAG from a variety of species (Poltorak et al., 1987; Tropak and Roder, 1994; Tropak et al., 1995), detected a single band of roughly 80 kDa in non-reduced, non-boiled tissue from rat brain and frog nerve (Fig. 3B). Similar results were obtained with mAb 3E4, except that there was an additional, higher molecular weight band, the significance of which is unclear. It appears that both mAbs detect MAG in *Rana pipiens* (see Discussion) and that MAG is not abundant in frog brain, as compared to frog nerve and rat brain. In summary, the immunoblot data reveal that the antibodies against P_0 and MAG identify the correct proteins in frog. Moreover, this indicates that the results obtained by immunohistochemistry also reflect detection of the proper myelin-related proteins.

PSCs Express GalC and CNPase

The major galactolipids of myelin are galactocerebroside (GalC) and its sulfated derivative galactosulfatide, and these are essential to myelin structure and function (for reviews see Stoffel and Bosio, 1997; Coetzee et al., 1998; Dupree et al., 1998). These molecules are regulated developmentally and both are expressed in mature myelin- and non-myelin-forming Schwann cells surrounding nerves (for review see Jessen and Mirsky, 1991). We detected GalC on PSCs and MSCs using a polyclonal antibody which binds GalC (Sigma; Benjamins et al., 1987; 12 sites from 2 muscles examined), the Ranscht mAb (R-mAb) which recognizes GalC and also sulfatide (Ranscht et al., 1982; 18 sites from 4 muscles examined), and mAb O1, which detects GalC (Sommer and Schachner, 1981; 12 sites from 2 muscles examined). A punctate staining pattern was obtained with the Ranscht and O1 mAbs, whereas the GalC polyclonal antibody uniformly stained PSCs (images not shown).

We also evaluated the distribution of 2′,3′-cyclic nucleotide-3′-phosphodiesterase (CNPase), a myelin-associated enzyme (for review see Sprinkle, 1989). Using a CNPase mAb (11–5B), we detected immunoreactivity at MSCs and PSCs. Although staining was weak, it appeared punctate along the length of PSCs, including the cytoplasm around their nucleus (18 sites from 2 muscles examined; images not shown). The results indicate that PSCs express the general myelin-forming cell markers GalC and CNPase.

DISCUSSION

In this study, we found that PSCs express the Schwann cell marker P_0, as well MAG, GalC, and CNPase, proteins abundant in myelin-forming glia. Previous studies showed that PSCs contain the Ca^{2+}-binding protein S100 (Reynolds and Woolf, 1992) and the glial fibrillary acidic protein (GFAP; Georgiou et al., 1994), which are abundant in glia but are also found in other cells. This molecular profile allows us to conclude that PSCs are likely of Schwann cell origin. P_0 and MAG each had unique distributions. P_0 was expressed

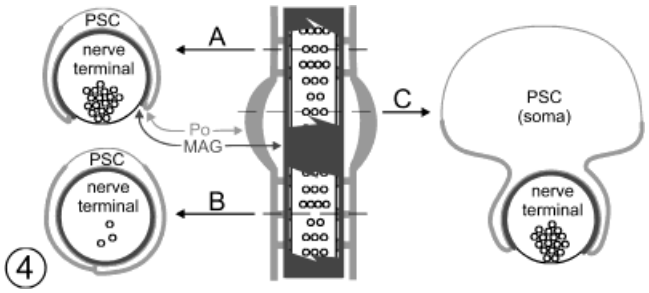

Fig. 4. Diagram of P_0 and MAG distribution on PSCs. The center diagram shows a section parallel to the muscle fibre, through a portion of a nerve terminal and the surrounding PSC. Synaptic vesicles are found in clusters at active zones, which occur at regularly spaced (1 μm) intervals along the nerve terminal. P_0 and MAG expression appear in a lighter and darker shade of gray, respectively. Note that P_0 is expressed over most of the PSC surface including extensions (fingers) reaching between the active zones. In contrast, MAG is primarily restricted to the contacting membrane regions between the nerve terminal and PSC. **A–C:** Cross-sections through selected regions (dashed arrows), comparing the cellular morphology and myelin-protein expression along the nerve terminal. A: An active zone region, showing synaptic vesicles clustered on the side of the nerve terminal membrane directly adjacent to the postsynaptic muscle cell (not shown). B: Section in which PSC fingers intervene between the nerve terminal and muscle cell. C: An active zone region sectioned through a PSC soma.

over most of the PSC membrane, including at the extensions that wrap around the nerve terminal at regions in between the active zones (Fig. 4). In contrast, MAG occurred primarily at contact areas of apposing nerve terminal-PSC membranes. P_0, and MAG persisted on PSCs and their extensions even after degeneration of the nerve terminals.

Characteristics of MAG and P_0

P_0 is the major protein in peripheral myelin, where it functions to hold together the layers of myelin membrane and to stabilize compact myelin (for review see Quarles, 1997; Martini and Schachner, 1997; Sommer and Suter, 1998). P_0 is expressed early in Schwann cell development and is now considered a marker for neural crest cells of the Schwann cell lineage (Bhattacharyya et al., 1991; Zhang et al., 1995; Lee et al., 1997; for review see Jessen and Mirsky, 1998).

P_0 has been found in many species, including frogs. In Western blots, anti-bovine P_0 antibodies found a band of about 35 kDa in *Rana catesbeiana* bullfrogs (Takei et al. 1993) and a more distinct band of roughly 33 kDa in *Rana temporaria* frogs (Jeserich and Waehneldt, 1987). We used *Rana pipiens* samples, which were not boiled or reduced, and found a wide band corresponding to a doublet of roughly 29 and 32 kDa. We also detected some P_0 in CNS extracts, which has been documented in some amphibian species (Takei and Uyemura, 1993). The greater mobility compared to previous studies is likely due to the use of more native conditions, which we found necessary for 1E8 reactivity. The loss of 1E8 immunoreactivity after boiling or reduction suggests that the P_0 epitope detected in frog is conformation-dependent, as it is in chicken (Zhang et al., 1995).

While there is an evolutionary conservation of P_0 in vertebrates, there are also differences between vertebrate classes. For instance, an anti-bovine antibody also detects P_0 in trout, frog, reptile, chick, and mouse, whereas an anti-trout antibody did not react in chicken and frog (Jeserich and Waehneldt, 1987). Moreover, the 1E8 mAb used in this study does not detect P_0 in mammals, but it does recognize P_0 in chickens, as well as in *Rana pipiens* frog, as we have now shown.

MAG is a 100 kDa glycoprotein localized in the periaxonal membranes of myelin-forming cells and appears to be important in the maintenance, rather than the formation, of myelin (for review see Quarles, 1997; Martini and Schachner, 1997). In our study, the MAG staining was narrower and primarily confined to within the PNA outline, and furthermore, staining usually did not expand to fill the PSC soma region. This pattern of staining is consistent with MAG being localized primarily at the PSC membrane adjacent to the nerve terminal (Fig. 4). However, we cannot exclude the possibility of MAG expression elsewhere, such as on the PSC membrane, which faces away from the nerve terminal, especially since permeabilization was required to visualize MAG. Because MAG affects axonal viability and cytoskeletal organization (Yin et al., 1998), it is plausible that nerve terminal structure and function are regulated by MAG found in the PSCs.

The MAG 513 mAb was obtained by immunizing mice with chicken brain glycoproteins (Poltorak et al., 1987), and it is known to bind MAG in a variety of tetrapod species, including mammals, birds, and Xenopus (Tropak et al., 1995). We found by Western blotting of brain samples from *Rana pipiens* that the 513 mAb recognizes a single protein of similar molecular weight to that of MAG from rat brain, suggesting that 513 also detects MAG in *Rana* (Fig. 3B). 513 only detects native MAG (Tropak and Roder, 1994) and this was confirmed by the fact that MAG could not be detected after rat and frog samples had been reduced and boiled (not shown). The mAb 3E4 also detected a band with similar mobility to that detected by 513 (Fig. 3C). Both antibodies appear to be specific probes for frog MAG.

Myelin-Protein Expression Persists After Denervation

P_0 and MAG are easily detected after degeneration of the nerve terminal. Therefore, it is clear that these proteins are expressed in PSCs. The pattern of staining was altered, and this may be a result of the change in PSC morphology, which occurred with nerve degeneration. For instance, PSCs engulf the degenerating nerve terminals and eventually fill the volume formerly occupied by the terminal (Birks et al., 1960b; Ko, 1981). Nevertheless, it is clear that these myelin proteins continue to be expressed in frogs two weeks after

denervation. Moreover, newly formed extensions of the PSC express P_0 and MAG.

Denervation and nerve activity blockade are known to induce alterations in PSC receptor characteristics and protein expression. For instance, PSC responses induced by muscarine have different pharmacological properties after denervation, suggesting that their complement of muscarinic acetylcholine receptors change (Robitaille et al., 1997). Denervation induces PSC expression of low affinity nerve growth factor receptor, growth-associated phosphoprotein GAP-43 (Reynolds and Woolf, 1992; Woolf et al., 1992), and 3G2/4E2 antigen (Astrow et al., 1994). PSCs also up-regulate GFAP after synaptic activity blockade (Georgiou et al., 1994), and GFAP remains elevated in PSCs from denervated muscles (unpublished observations). Activation of PSC muscarinic acetylcholine receptors can prevent GFAP up-regulation induced by nerve transection (Georgiou et al., 1999). Alterations in PSC protein expression may relate to the new glial activities that occur after denervation, such as phagocytosis of nerve terminals (Birks et al., 1960b), release of acetylcholine (Birks et al., 1960b; Bevan et al., 1973), glial process extension (Reynolds and Woolf, 1992), and guidance of neurons (Son et al., 1995a; 1995b).

Expression of P_0 and MAG persisted in PSCs after denervation, which is in contrast to the effect of denervation on MSCs (for review see Scherer, 1997). Another protein expressed in PSCs from rat neuromuscular junctions, and which persists after denervation, is S100 (Reynolds and Woolf, 1992). Because S100, P_0, and MAG are still present after denervation, their expression in PSCs appears to be independent of axonal factors or contact.

Lack of Myelination at PSCs and Roles of P_0 and MAG

Although PSCs express proteins thought to be critical for myelination, they do not form myelin. The diameter of the axon terminals is not any smaller than that of the same innervating myelinated axons (personal observations; McMahan et al., 1972), and thus, it is unlikely that terminals are too thin to allow for myelination. Instead, the ability of PSCs to form myelin might be inhibited by action of neurotransmitters on PSC receptors. Another possibility is that extracellular protein factors at the synapse prevent myelination. For instance, interference with extracellular matrix glycoproteins, such as cytotactin/tenascin, the neural cell adhesion molecule, and laminin, affects the neuromuscular synapse, re-innervation and PSCs (Rieger et al., 1988; Mège et al., 1992; Langenfeld-Oster et al., 1994; Cifuentes-Diaz et al., 1998; Patton et al., 1998).

The roles of P_0 and MAG in PSCs may relate to nerve–glial interactions, such as adhesion and synaptic plasticity. For instance, these glycoproteins contain the carbohydrate epitope L2/HNK-1, which is shared by adhesion molecules and is involved in homophilic binding of P_0, and possibly heterophilic interactions (for reviews see Quarles, 1997; Martini and Schachner, 1997; Sommer and Suter, 1998). P_0 and MAG may thus be required for continual glial plasticity, or other functions related to PSC adhesion. It may be possible to test whether these glycoproteins participate in glial–synapse interactions by applying antibodies to interfere with these proteins or by examining neuromuscular junctions in mice that are deficient in these molecules.

ACKNOWLEDGMENTS

We thank Dr. Robert Brackenbury and Dr. Nancy Ratner (University of Cincinnati College of Medicine), Dr. John C. Roder (Samuel Lunenfeld Research Institute, Mt. Sinai Hospital, Toronto, Canada), and Dr. Barbara Ranscht (The Burnham Institute, La Jolla Cancer Research Center) for antibodies. We also thank Dr. Tropak for his advice and for reading the manuscript, and Dr. Donald B. Elrick for his comments.

This work was supported by a Medical Research Council of Canada Group Grant "Nerve Cells and Synapses" to M.P.C. and by the Neuroscience Network. J.G. was supported by a Neuroscience Network Studentship.

REFERENCES

Anderson MJ, Cohen MW. 1974. Fluorescent staining of acetylcholine receptors in vertebrate skeletal muscle. J Physiol (Lond) 237:385–400.

Astrow SH, Son YJ, Thompson WJ. 1994. Differential neural regulation of a neuromuscular junction-associated antigen in muscle fibers and Schwann cells. J Neurobiol 25:937–952.

Balice-Gordon RJ 1996. Schwann cells: dynamic roles at the neuromuscular junction. Curr Biol 6:1054–1056.

Benjamins JA, Callahan RE, Montgomery IN, Studzinski DM, Dyer CA. 1987. Production and characterization of high titer antibodies to galactocerebroside. J Neuroimmunol 14:325–338.

Bevan S, Miledi R, Grampp W. 1973. Induced transmitter release from Schwann cells and its suppression by actinomycin D. Nat New Biol 241:85–86.

Bhattacharyya A, Frank E, Ratner N, Brackenbury R. 1991. P_0 is an early marker of the Schwann cell lineage in chickens. Neuron 7:831–844.

Birks R, Huxley HE, Katz B. 1960a. The fine structure of the neuromuscular junction of the frog. J Physiol (Lond) 150:134–144.

Birks R, Katz B, Miledi R. 1960b. Physiological and structural changes at the amphibian myoneural junction in the course of nerve degeneration. J Physiol (Lond) 150:145–168.

Bourque M-J, Robitaille R. 1998. Endogenous peptidergic modulation of perisynaptic Schwann cells at the frog neuromuscular junction. J Physiol (Lond) 512:197–209.

Burden SJ. 1998. The formation of neuromuscular synapses. Genes Dev 12:133–148.

Cifuentes-Diaz C, Velasco E, Meunier FA, Goudou D, Belkadi L, Faille L, Murawsky M, Angaut-Petit D, Molgó J, Schachner M, Saga Y, Aizawa S, Rieger F. 1998. The peripheral nerve and the neuromuscular junction are affected in the tenascin-C-deficient mouse. Cell Mol Biol (Noisy-le-grand) 44:357–379.

Coetzee T, Suzuki K, Popko B. 1998. New perspectives on the function of myelin galactolipids. Trends Neurosci 21:126–130.

Doyle JP, Colman DR. 1993. Glial–neuron interactions and the regulation of myelin formation. Curr Opin Cell Biol 5:779–785.

Dreyer F, Peper K. 1974. A monolayer preparation of innervated skeletal muscle fibres of the M. cutaneus pectoris of the frog. Pflügers Arch 348:257–262.

Dreyer F, Peper K, Akert K, Sandri C, Moor H. 1973. Ultrastructure of the 'active zone' in the frog neuromuscular junction. Brain Res 62:373–380.

Dupree JF, Suzuki K, Popko B. 1998. Galactolipids in the formation and function of the myelin sheath. Microsc Res Tech 41:431–440.
Georgiou J, Robitaille R, Trimble WS, Charlton MP. 1994. Synaptic regulation of glial protein expression in vivo. Neuron 12:443–455.
Georgiou J, Robitaille R, Charlton MP. 1999. Muscarinic control of cytoskeleton in perisynaptic glia. J Neurosci 19 (in press).
Hall ZW, Sanes JR. 1993. Synaptic structure and development: the neuromuscular junction. Cell 72 / Neuron 10 (Suppl):99–121.
Heuser JE, Reese TS. 1977. Structure of the synapse. In: Brookhart JM, Mountcastle VB, Kandel ER, Geiger SR, editors. Handbook of physiology: the nervous system. Baltimore: Waverly Press. p 261–294.
Jahromi, BS, Robitaille R, Charlton MP. 1992. Transmitter release increases intracellular calcium in perisynaptic Schwann cells in situ. Neuron 8:1069–1077.
Jeserich G, Waehneldt, TV. 1987. Antigenic sites common to major fish myelin glycoproteins (IP) and to major tetrapod PNS myelin glycoprotein (P_0) reside in the amino acid chains. Neurochem Res 12:825–829.
Jessen KR, Mirsky R. 1998. Origin and early development of Schwann cells. Microsc Res Tech 41:393–402.
Jessen KR, Mirsky R. 1991. Schwann cell precursors and their development. Glia 4:185–194.
Ko C-P. 1981. Electrophysiological and freeze-fracture studies of changes following denervation at frog neuromuscular junctions. J Physiol (Lond) 321:627–639.
Ko C-P. 1987. A lectin, peanut agglutinin, as a probe for the extracellular matrix in living neuromuscular junctions. J Neurocytol 16:567–576.
Langenfeld-Oster B, Faissner A, Irintchev A, Wernig A. 1994. Polyclonal antibodies against NCAM and tenascin delay endplate reinnervation. J Neurocytol 23:591–604.
Le Douarin N, Dulac C, Dupin E, Cameron-Curry P. 1991. Glial cell lineages in the neural crest. Glia 4:175–184.
Lee M-J, Brennan A, Blanchard A, Zoidl G, Dong Z, Tabernero A, Zoidl C, Dent MAR, Jessen KR, Mirsky R. 1997. P_0 is constitutively expressed in the rat neural crest and embryonic nerves and is negatively and positively regulated in axons to generate non-myelin-forming and myelin-forming Schwann cells, respectively. Mol Cell Neurosci 8:336–350.
Martini R, Schachner M. 1997. Molecular bases of myelin formation as revealed by investigations on mice deficient in glial cell surface molecules. Glia 19:298–310.
McMahan UJ, Spitzer NC, Peper K. 1972. Visual identification of nerve terminals in living isolated skeletal muscle. Proc R Soc Lond B 181:421–430.
Mège RM, Nicolet M, Pinçon-Raymond M, Murawsky M, Rieger F. 1992. Cytotactin is involved in synaptogenesis during regeneration of the frog neuromuscular system. Dev Biol 149:381–394.
Patton BL, Chiu AY, Sanes JR. 1998. Synaptic laminin prevents glial entry into the synaptic cleft. Nature 393:698–701.
Poltorak M, Sadoul R, Keilhauer G, Landa C, Fahrig T, Schachner M. 1987. Myelin-associated glycoprotein, a member of the L2/HNK-1 family of neural cell adhesion molecules, is involved in neuron-oligodendrocyte and oligodendrocyte-oligodendrocyte interaction. J Cell Biol 105:1893–1899.
Quarles RH. 1997. Glycoproteins of myelin sheaths. J Mol Neurosci 8:1–12.
Ranscht B, Clapshaw PA, Price J, Noble M, Seifert W. 1982. Development of oligodendrocytes and Schwann cells studied with a monoclonal antibody against galactocerebroside. Proc Natl Acad Sci USA 79:2709–2713.
Reist NE, Smith SJ. 1992. Neurally evoked calcium transients in terminal Schwann cells at the neuromuscular junction. Proc Natl Acad Sci USA 89:7625–7629.
Reynolds ML, Woolf CJ. 1992. Terminal Schwann cells elaborate extensive processes following denervation of the motor endplate. J Neurocytol 21:50–66.
Rieger R, Nicolet M, Pinçon-Raymond M, Murawsky M, Levi G, Edelman GM. 1988. Distribution and role in regeneration of N-CAM in the basal laminae of muscle and Schwann cells. J Cell Biol 107:707–719.
Robitaille R. 1995. Purinergic receptors and their activation by endogenous purines at perisynaptic glial cells of the frog neuromuscular junction. J Neurosci 15:7121–7131.
Robitaille R. 1998. Modulation of synaptic efficacy and synaptic depression by glial cells at the frog neuromuscular junction. Neuron 21:847–55.
Robitaille R, Adler EM, Charlton MP. 1990. Strategic location of calcium channels at transmitter release sites of frog neuromuscular synapses. Neuron 5:773–779.
Robitaille R, Bourque M-J, Vandaele S. 1996. Localization of L-type Ca^{2+} channels at perisynaptic glial cells of the frog neuromuscular junction. J Neurosci 16:148–158.
Robitaille R, Jahromi BS, Charlton MP. 1997. Muscarinic Ca^{2+} responses resistant to muscarinic antagonists at perisynaptic Schwann cells of the frog neuromuscular junction. J Physiol (Lond) 504:337–347.
Scherer SS. 1997. The biology and pathobiology of Schwann cells. Curr Opin Neurol 10:386–397.
Sommer I, Schachner M. 1981. Monoclonal antibodies (O1 to O4) to oligodendrocyte cell surfaces: an immunocytological study in the central nervous system. Dev Biol 83:311–327.
Sommer L, Suter U. 1998. The glycoprotein P0 in peripheral gliogenesis. Cell Tissue Res 292:11–16.
Son Y-J, Thompson WJ. 1995a. Schwann cell processes guide regeneration of peripheral axons. Neuron 14:125–132.
Son Y-J, Thompson WJ. 1995b. Nerve sprouting in muscle is induced and guided by processes extended by Schwann cells. Neuron 14:133–141.
Son Y-J, Trachtenberg JT, Thompson WJ. 1996. Schwann cells induce and guide sprouting and reinnervation of neuromuscular junctions. Trends Neurosci 19:280–285.
Sprinkle TJ. 1989. 2′,3′-cyclic nucleotide 3′-phosphodiesterase, an oligodendrocyte-Schwann cell and myelin-associated enzyme of the nervous system. Crit Rev Neurobiol 4:235–301.
Stoffel W, Bosio A. 1997. Myelin glycolipids and their functions. Curr Opin Neurobiol 7:654–661.
Takei K, Uyemura K. 1993. Expression of a P0-like glycoprotein in central nervous system myelin of amphibians (*Ambystoma mexicanus*, *Xenopus laevis* and *Rana catesbeiana*). Comp Biochem Physiol 106B:873–882.
Takei K, Kitamura K, Banno K, Uyemura K. 1993. Major glycoproteins in carp CNS myelin: homology to P0 protein with HNK-1/L2 carbohydrate epitope. Neurochem Int 23:239–248.
Tropak MB, Roder JC 1994. High-resolution mapping of GenS3 and B11F7 epitopes on myelin-associated glycoprotein by expression PCR. J Neurochem 62:854–862.
Tropak MB, Jansz GF, Abramow-Newerly W, Roder JC. 1995. Conservation of functionally important epitopes on myelin associated glycoprotein (MAG). Comp Biochem Physiol 112B:345–354.
Woolf CJ, Reynolds ML, Chong MS, Emson P, Irwin N, Benowitz LI. 1992. Denervation of the motor endplate results in the rapid expression by terminal Schwann cells of the growth-associated protein GAP-43. J Neurosci 12:3999–4010.
Yin X, Crawford TO, Griffin JW, Tu P-H, Lee VM-Y, Li C, Roder J, Trapp BD. 1998. Myelin-associated glycoprotein is a myelin signal that modulates the caliber of myelinated axons. J Neurosci 18:1953–1962.
Zhang S-M, Marsh R, Ratner N, Brackenbury R. 1995. Myelin glycoprotein P_0 is expressed at early stages of chicken and rat embryogenesis. J Neurosci Res 40:241–250.